AIRFLOW PATTERN AND PERFORMANCE ANALYSIS OF DIFFUSE CEILING VENTILATION IN AN OFFICE ROOM USING CFD STUDY

Chen Zhang[1], Qingyan Chen[2], Per K. Heiselberg[1], Michal Z. Pomianowski[1]
[1]Department of Civil Engineering, Aalborg University, Aalborg, 9200, Denmark
[2]School of Mechanical Engineering, Purdue University, West Lafayette, IN 47907, USA

ABSTRACT

Diffuse ceiling ventilation uses perforations in the suspended ceiling to deliver air into the occupied zone. Due to the complex geometry of the diffuser, it is not possible to build an exact geometrical model in CFD simulation. Two numerical models are proposed in this study, one is a simplified geometrical model and the other is a porous media model. The numerical models are validated by the full-scale experimental studies in a climate chamber. The results indicate that porous media model performed better on predicting air flow characteristic below diffuse ceiling and air velocity near the floor. However, the simplified geometrical model shows superior performance on calculating the diffuse ceiling surface temperature.

INTRODUCTION

The diffuse ceiling ventilation is an air distribution concept where the space above a suspended ceiling is used as a plenum and fresh air is supplied into the occupied zone through perforations in the suspended ceiling panels. As the large ceiling area serves as the supply opening, airflow is delivered into the occupied zone with very low velocity and with no fixed jet direction, hence the name 'diffuse'. The flow pattern in the room is normally controlled by the buoyance flow generated by heat sources. This ventilation concept was widely used in livestock buildings due to its low investment cost and high thermal comfort level(Jacobsen, 2008) (Rong, Elhadidi, Khalifa, & Nielsen, 2010.) as well as in clean rooms where high ventilation effectiveness is required (Brohus & Balling, 2004). In recent years, the applications and studies regarding utilization of diffuse ceiling ventilation in indoor spaces for humans are increasing gradually, especially for offices and classrooms with high heat loads and high ventilation demands.

The performance of diffuse ceiling ventilation in an office room was investigated by Nielsen et al. (2007) (Jakubowska, 2007) and compared with five other air distribution systems. Their investigations showed that diffuse ceiling ventilation presented superior performance on handling high heat loads with low draught risk in the occupied zone. Hviid et al. (2013) performed an experimental study in a climate chamber with two perforated tiles as diffuse ceiling supply. The results were in good agreement with Nielsen's and no local discomfort in the occupant zone was found and the air change efficiency was comparable to mixing ventilation. On the other hand, they pointed out that a low pressure drop of 0.5 Pa to 1.5 Pa is enough to sustain the pressure of the plenum and ensure uni-directional flow through diffuse ceiling and that there is a radiation cooling potential of the ceiling. The other advantages such as modest investment costs, low energy consumption and low noise level was reported by Jacobs et al.(2009) from a pilot study in a classroom.

Studies of ventilation systems mainly use two approaches: experimental and numerical study. Compared with an experimental study, the numerical study is reputed for its low cost and time efficiency, as the boundary conditions can be easily changed to study different scenarios. The geometry of the diffuse ceiling diffuser is too complicated to be directly modelled in practical CFD-simulations. Therefore, simplified models that aim to describe the main characteristic of the diffuse ceiling ventilation needs to be developed.

Simplified models for some other supply diffusers have been extensively studied and been validated, such as momentum model and box model. In the momentum model, an initial jet momentum is imposed as a source term, and momentum and mass boundary conditions for the diffusers are decoupled for CFD simulations (Chen & Moser, 1991) (Srebric & Chen, 2003). The box method is conducted by defined the boundary conditions on an imaginary box surface around the diffuser(Skovgaard, M., Nielsen, 1991). One difficulty of this method is to specify the box size, which should have the boundaries in the fully developed region and avoid the impact of room air recirculation. On the other hand, in order to specify the boundary condition, either suitable jet relation or extensive measurement data is required. However, due to the unique properties of diffuse ceiling, these methods cannot effectively describe the air flow pattern and the flow characteristics of diffuse ceiling ventilation. First of all, the large ceiling area is used as supply diffuser, where the fully developed jet relation is not applicable and the measurement of the box boundary condition is unrealistic. Secondly, the use of a ceiling plenum to deliver air is one of the key features that distinguish diffuse ceiling ventilation from the conventional ducted air distribution system. The heat exchange between supply air and the thermal mass in the plenum will

influence the supply air temperature as it passing through the plenum. Therefore, the air will be supplied with non-uniform temperature and non-uniform amount through the diffuser. Although momentum method could introduce a correct momentum flow, it is impossible to predict the air temperature distribution and velocity distribution at the inlet boundary. Finally, the configurations of plenum and properties of diffuse ceiling panels have strong influence on the effectiveness of diffuse ceiling ventilation, and these parameters should be taken into account in the numerical model. Therefore, a simplified model needs to be established to effectively simulate diffuse ceiling ventilation.

Several numerical studies on diffuse ceiling ventilation haven been reported. Fan et al. (2013) simplified the diffuse ceiling as 4 long rectangular strips with the same effective area. They pointed out there is a slightly disagreement between numerical and experimental results due to the simplification of ceiling air passage, which cause overestimation/ underestimation of air movement in the room, especially in the region close to the ceiling. In Chodor's study (2013), they neglected the impact of the plenum and assumed the air was uniform distributed through the entire ceiling area with outdoor air temperature and with superficial velocity. Hviid (2013) had the similar assumption in his simulation. These studies focus on the characteristics of airflow in the conditioned space, however, the air distributed in the plenum and air flow through diffuse ceiling is not discussed in detail.

The purpose of this study is to propose a numerical model, which could effectively describe the air flow pattern of diffuse ceiling ventilation in both plenum and occupied zone. Two simplified models are built and compared, one is a simplified geometrical model and the other is a porous media model. The thermal comfort in the occupied zone is estimated by the temperature gradient and the velocity profile at different locations in the conditioned space. The air flow pattern in the plenum and through the diffuse ceiling is evaluated by the temperature distribution of plenum air and on the upper and lower surface of diffuse ceiling panel. Radiant ceiling system will work as a supplementary system to deal with additional heating or cooling demand during winter and summer. The impact of radiation on the accuracy of simplified models is also discussed. The numerical models are validated by experimental studies in different operating conditions.

EXPERIMENTAL DESCRIPTION

Diffuse ceiling and its physical properties

In this study, the diffuse ceiling is made by cement-wood panels, which are originally used for sound absorption, as shown in Figure 1. Each panel has the dimension of 35 mm in thickness, 600 mm in width and 1200 mm in length. The density of the ceiling panel is measured to be 359.13 kg/m^3. The porosity is estimated through volumetric measurement, which is 65%. The thermal conductivity is measured by λ-Meter EP500 based on the guarded hot plate method, and the value is 0.085 W/m.K with a measurement error less than 1.0 %.

The pressure drop across the ceiling panel is measured as function of superficial velocity. The panel sample is placed in the centre of a pressure chamber, and the pressure difference across the sample is measured by FCO 510 micromanometer with an accuracy of 0.25%. The results are shown in Figure 2, indicated as pressure drop across a single panel.

Figure 1 Cement-wood panel

Figure 3 Diffuse ceiling setup

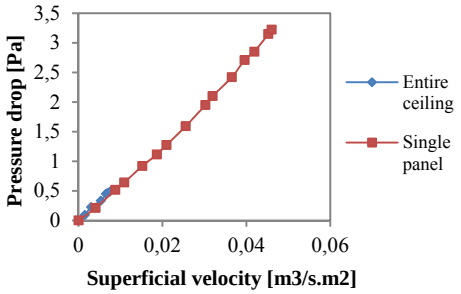

Figure 2. Function between pressure drop and superficial velocity for single panel and entire ceiling

Test chamber

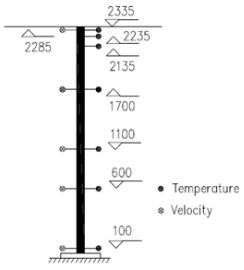

Figure 4 Temperature and velocity sensors in the moveable columns

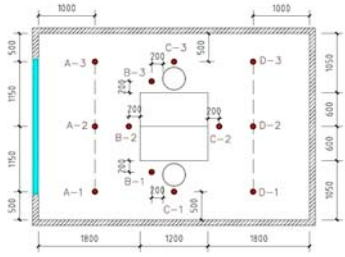

Figure 5 Measurement locations of air temperature and velocity in the conditioned space

In order to investigate the airflow pattern in the room with diffuse ceiling ventilation, a test system is installed in a climate chamber with a dimension of 4.8m * 3.3m * 2.72m (length * width * height). The diffuse ceiling is installed 0.35 m below the ceiling

concrete slab and is fixed by suspension profiles, as illustrated in Figure 3. The suspended ceiling panels cover the entire ceiling area and separate the space into two zones: the plenum and the conditioned space. The air is supplied into the plenum through three small windows located above the diffuse ceiling, with a geometric opening area of 0.0675 m^2. The exhaust is located in the conditioned space, at the bottom left corner of the front wall with a diameter of 160 mm. The air is drawn from the test chamber into a connected cooling chamber by means of an exhaust fan, and it will be re-supplied into the test chamber after cooling down by the air-handling unit located inside the cooling chamber.

The test room is set up to represent an office layout. Two workplaces are arranged, which consists of two desks with two computers (55W and 45 W), two monitors (16 W and 21.5 W) and two task lamps (54 W and 59 W). Two persons are simulated by thermal manikins (100 W for each). The overall heat load is 450.5 W (28.44 W/m2).

In the experiments, the air velocity and air temperature are measured in both plenum and conditioned space. Three moveable columns are located in the occupied zone, and in each column there are 7 thermocouples and 5 anemometers positioned at different heights to measure vertical temperature and velocity profiles, as indicated in Figure 4. Each column are moved to 4 positions, so that in total 12 positions have been measured in the occupied zone, as indicated in Figure 5. In the plenum, the thermocouples and anemometers are placed in the central line, at three different distances to the inlet (0.8 m, 2.4 mand 4.0 m). In addition, the surface temperature of diffuse ceiling panels and inner walls are measured. The temperatures are measured by K-type thermocouples with an accuracy of ± 0.15 K. The air velocities are measured by Dantec 54R 10 Hot sphere anemometer with a accuracy of ± 0.01 m/s +5% of reading. Finally, there are 5 pressure sensors located in the plenum and the conditioned space to determine the pressure drop across the diffuse ceiling and the pressure difference is recorded by FCO510 micromanometer.

Table 1

Test conditions in three scenarios

Case	ACH h^{-1}	Supply air temp ^oC	Slab surface temp ^oC	Heat load W
1	2	9.46	-	450.5
2	2	24.10	10.79	450.5
3	2	-6.87	27.34	450.5

Note: In scenario 1 where radiant slabs are not activated, slab surface temperature reacts to the air temperature and other wall temperatures. In scenarios 2 and 3, radiant slabs are activated and the slab surface temperature is controlled by water temperature.

Experiments are carried out in three scenarios with a supply air temperature range of 24.1 ^oC to -6.8 ^oC, which represents diffuse ceiling ventilation operating conditions at different seasons. A constant air change rate of 2 h^{-1} and a constant heat load of 450.5 W are used in all three scenarios. In order to keep an acceptable indoor environment, radiant slabs located above the diffuse ceiling serve as a supplementary system to deal with additional heating or cooling demand. The detail test conditions are listed in Table 1.

NUMERICAL MODEL

Simplified geometrical model

The simplified geometrical model approach is the most common method to simulate an air diffuser. The inlet boundary is set by reducing the inlet opening size, which is easy to implement in the CFD model. Heikkinen et al.(1993) pointed out that this method can produce good results for regions remote from the initial jet development.

Due to the special structure of the cement-wood panel (Figure 1), the effective opening area ratio of the diffuse ceiling does not equal to the panel's porosity and is difficult to be measured directly. Therefore, the effective opening area is calculated based on the pressure drop results obtained by measurement, as expressed by Eq (1).

$$C_d A = \frac{\dot{m}}{\sqrt{2\rho\Delta P}} \quad (1)$$

Where: ṁ is the mass flow rate, ΔP is the pressure drop across the diffuse ceiling, C_d is the discharge coefficient. A default C_d value of 0.6 is used in this study, which is suitable for the opening with low area ratio. Therefore, three slots opening with an effective area of 0.032 m^2 each are built to simulate the air passage of diffuse ceiling ventilation, as illustrated in Figure 6 (a).

The thermal process within the plenum is complex, which includes both the convective heat exchange between supply air and thermal mass and radiative heat exchange between diffuse ceiling panels and radiant slabs. Therefore, a surface-to-surface radiation model is activated in this model.

Porous media model

Due to the material properties of the wood-cement panel, a porous media model is adopted to simulate the flow through diffuse ceiling, as shown in Figure 6 (b). The basic idea of porous media model is to add a momentum sink in the governing momentum equation. The source term is composed of two parts: a viscous loss term and an inertial loss term(ANSYS, 2009). In laminar flows through porous media, the pressure drop is typically proportional to velocity, while at high flow velocity, the inertial loss will be dominant in the porous media, as expressed by Eq (2).

$$S_i = -\left(\frac{\mu}{\alpha} v_i + C_2 \frac{1}{2} \rho |v| v_i\right) \quad (2)$$

Where: v represent superficial velocity, α is the permeability, C_2 is inertial resistance factor. The viscous and inertial resistance coefficient $1/\alpha$ and C_2 are determined based on the function between pressure loss through porous media and superficial velocity obtained by experiments. In the experimental study, both the pressure drop across a single panel and the pressure drop across the entire ceiling are measured, as shown in Figure 2. Due to the large ceiling area and the limited capacity of the exhaust fan, only the small superficial velocities are performed when measured the entire ceiling pressure loss. The linear function between pressure drop and superficial velocity indicates the flow is laminar when it goes through the ceiling. These two pressure drop profiles correspond well with each other, revealing a fact that the cracks between ceiling panels and suspension system do not have apparent impact on the pressure drop. The viscous resistance and inertia resistance are calculated to be 1.14 e^{+8} m^{-2} and 33055 m^{-1}, respectively.

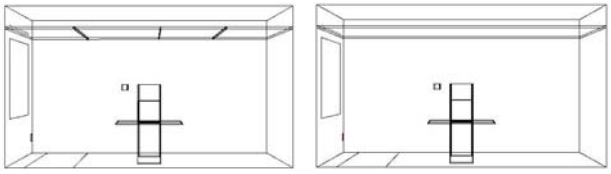

(a) (b)

Figure 6 CFD model of the office room with diffuse ceiling (a) Simplified geometry model (b) Porous media model

The energy equation in porous media is modified on the conduction flux and the transient terms only, as expressed by Equation (3). An effective thermal conductivity of the medium is introduced as the volume average of the fluid conductivity and the solid conductivity.

$$\frac{\partial}{\partial t}\left(\gamma \rho_f E_f + (1-\gamma)\rho_s E_s\right) + \nabla \cdot \left(\vec{v}\left(\rho_f E_f + P\right)\right) = \nabla \cdot \left[k_{eff} \nabla T - \left(\sum h_i J_i\right) + \left(\bar{\tau} \cdot \vec{v}\right)\right] + S_f \quad (3)$$

Where: E_f is the total fluid energy, E_s is the total solid medium energy, γ is the porosity of the medium, and k_{eff} is the effective thermal conductivity of the medium.

Unfortunately, the porous media model is incompatible with radiation model because it is regarded as a fluid zone and the diffuse ceiling surfaces are treated as interiors between two fluid zones. In order to overcome this limitation, a radiation model is built separately, where the porous media is replaced by a solid material with the same thermal properties. The calculated surface temperatures (except diffuse ceiling surface temperature) is directly used as boundary inputs in the porous media model and heat exchanges between porous media zone and the other zones (plenum and room) are calculated and treated as an energy source term S_f in the energy equation (3).

Turbulence model and Boundary conditions

As mentioned, the air flow through the diffuse ceiling with very low velocity and the flow is laminar. However, the convection air flow generated by the heat sources in the occupied zone increase the turbulence level. Thus, the Re-normalized group (RNG) k-ε model is appropriate for this situation, which provides an analytically derived differential formal for effective viscosity for low-Reynolds-number effects compared with the standard k-ε model (ANSYS, 2009). The boussinesq hypothesis is selected to model buoyancy-driven flow, with air thermal expansion coefficient of $0.343*10^{-3}$ K^{-1}.

The geometrical model is created to represent the test chamber as it is physically, as shown in Figure 6. The entire model is divided into three zones: plenum, diffuse ceiling and room. As mentioned, three small windows above diffuse ceiling serves as inlet and a ventilation duct located in the same wall serves as outlet in the experiment. In order to simplify the geometrical model and generate a high quality mesh, the inlet and outlet are simplified as rectangular openings with the same area in the CFD model. The inlet is assumed to have a uniform profile, where the air temperature and velocity are kept the same as in the experiments. The outlet is simulated with zero pressure and zero gradient conditions for all the flow parameters.

The U-values of the walls are used as input for all the wall boundaries, and the measured air temperature in the cooling chamber and the surrounding zone are used as free stream temperatures. The heat released by heat sources consists of convection and radiation. For the model with radiation, the total heat loads are released from heat sources as surface heat fluxes. For porous media model where radiation is not compatible, the effect of radiation heat exchange has been presented on the surface temperature of enclosed walls. Therefore, only the convection heat flow boundary condition is specified for the heat sources.

Numerical methods

Mesh is an important factor for the high quality CFD model. The general idea is that fine grids must be used in areas with large gradients to minimize false diffusion and dispersive errors. In this study, structured meshes are generated in the entire computational domain and the finest meshes are generated in critical areas such as: diffuse ceiling, inlet, outlet, area closed to the walls and heat sources. A grid independency study is performed by models with different mesh densities. The total number of cells needed is determined to be 741,831for the simplified geometrical model and 669,262 for the porous media model.

The SIMPLE numerical algorithm is used. The criteria of convergence is set such that the residuals for *u, v, w, k, ε* less than 10^{-3}, and the residual for energy less than 10^{-6}.

RESULTS AND DISCUSSIONS

Air flow pattern in the conditioned space

Figure 7 and 8 illustrate the velocity and temperature distribution at the central plane of the office room in scenario 1. The air flow pattern predicted by the two models show a similar trend. The thermal plume generated by heat sources is the dominant driven force in the room with diffuse ceiling ventilation. The uprising buoyance flow above heat sources and the downward flow attached the wall generate air circulations in the room. Small jet flows below diffuse ceiling are observed in the simplified geometrical model, but its effect to the air flow pattern in the conditioned space is negligible compared to the buoyance driven flow. Relatively high air velocities are found at the ankle level in both models. However, the simplified geometrical model predicts high ankle velocities in both sides of the room, while, the porous media model indicates high ankle velocity mainly occurs in the side closed to the front wall (left side).

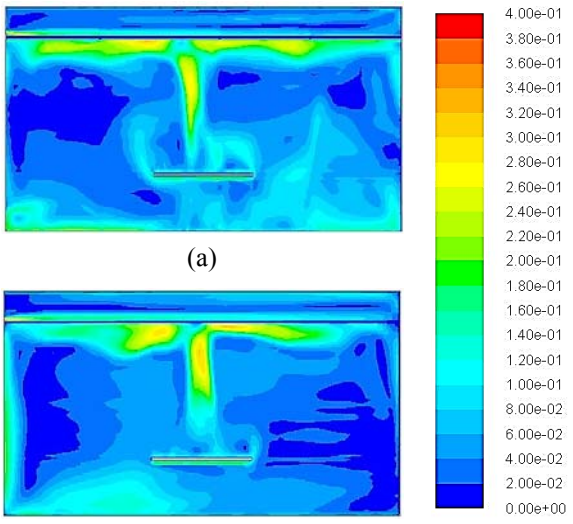

(a)

(b)

Figure 7 Velocity contour across the central plane of the room (a) Simplified geometrical model (b) Porous media model

The positive pressure in the plenum relative to the room enable air mixing in the plenum before it is supplied into the room and diffuse ceiling panels serve as a layer of insulation between the plenum and the conditioned space. Therefore, an air temperature difference between the plenum and the conditioned space will be expected, as shown in Figure 8. However, the air temperature is not uniform in the plenum due to its heat exchange with thermal mass (concrete slab and diffuse ceiling panel). The supply air temperature varies as a function of distance travelled through the plenum. Although air is supplied through the diffuse ceiling diffuser with non-uniform temperature, its impact on the room air temperature distribution is not obvious. The air temperature is predicted to be uniformly distributed in the occupied zone (except the region above heat sources), because of convection flows generated by the heat sources increases the mixing level.

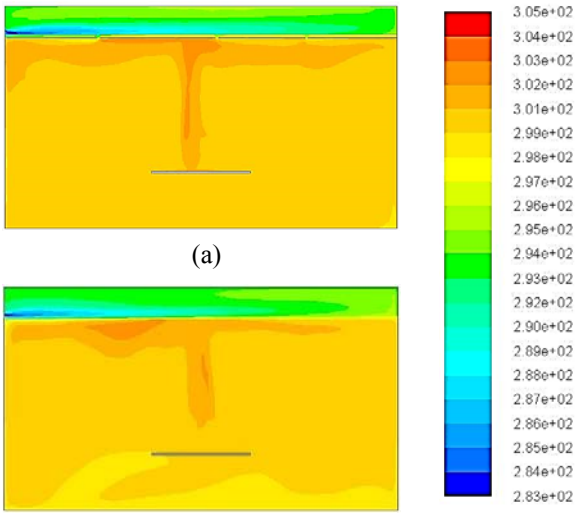

(a)

(b)

Figure 8 Temperature contour across the central plane of the room (a) Simplified geometrical model (b) Porous media model

Figure 9 and 10 show the vertical profiles of air temperature and velocity at four locations in the chamber, comparing the CFD modelling results with the measurement results. Although measurements are taken in many locations, the four locations along the central panel of the room are selected because they can represent the air flow characteristics in the room with diffuse ceiling ventilation. As indicated by Figure 9, a low vertical air temperature gradient is observed in the occupied zone. The temperature difference are less than 0.7 ^{o}C between the head and ankle level in all locations, which are much less than the limitation of 3 K required by ISO 7730 category B(ISO 7730, 2005). A good agreement has been reached between the computed air temperature and measured data in the occupied zone. The largest discrepancy is found in the region below the diffuse ceiling, where the CFD models overestimate the effect of the thermal plume. Compared with the simplified geometrical model, the porous media model gives a better prediction of the air temperature below diffuse ceiling, especially in location C-2 and D-2. This is because the porous media model allows air supply through the entire ceiling area, which is more close to the realistic air flow characteristics of diffuse ceiling ventilation.

Figure 10 indicates that the air velocity in the occupied zone is generally low, and no draught risk

is observed in all locations. A relatively high velocity is found at the ankle level closed to the front wall (A-2). The air velocity near the floor gradually reduces with increasing distance to the front wall. The porous media model show better performances on predicting the air velocity. The simplified geometrical model overestimate the air velocity near the floor and the velocity at location D-2. Both models indicate there is a peak velocity 5-10 cm below the diffuse ceiling, due to the thermal plume. More measured data is required in this region to validate this finding.

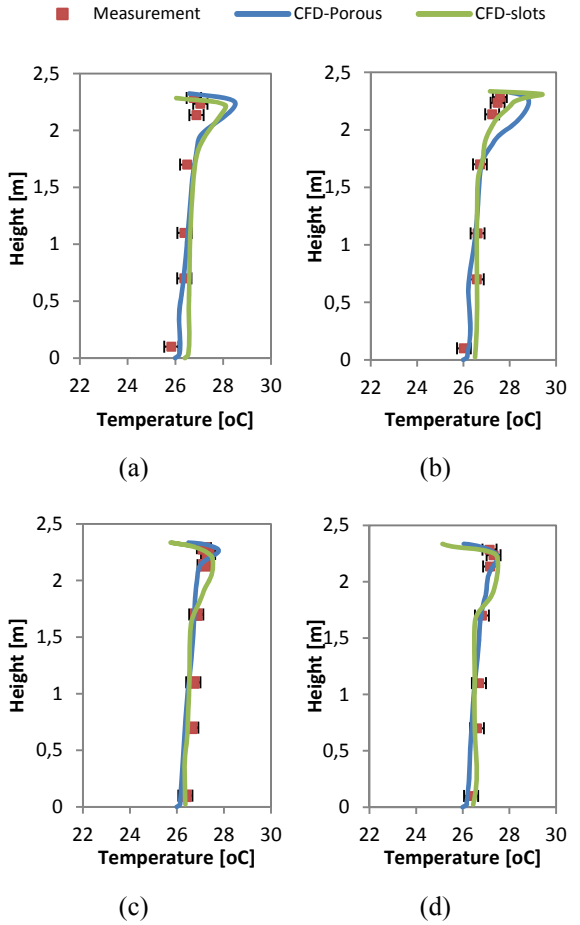

Figure 9 Comparison of the vertical temperature profile at different locations for scenario 1 (a) A-2 (b) B-2 (c) C-2 (d) D-2

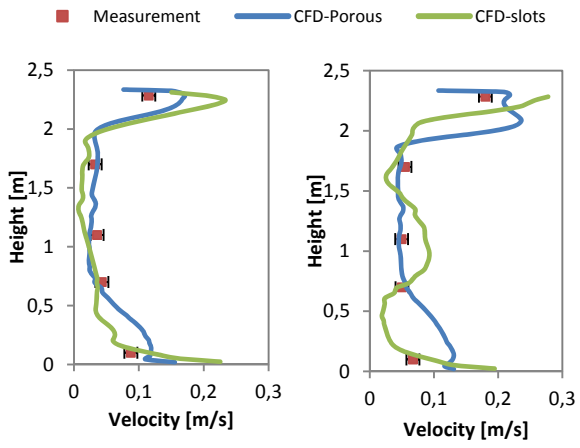

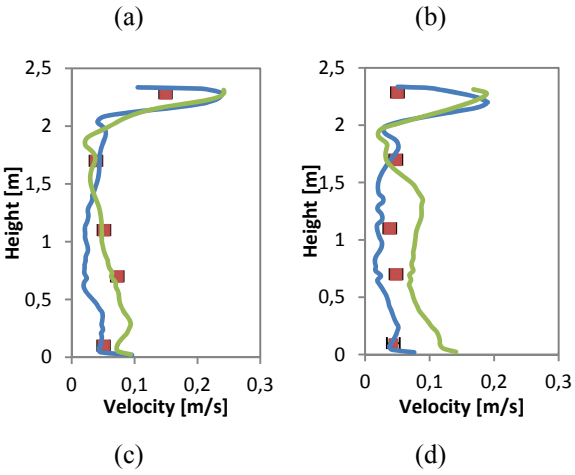

Figure 10 Comparison of the vertical velocity profile at different locations for scenario 1 (a) A-2 (b) B-2 (c) C-2 (d) D-2

Scenario 2 simulates a summer condition and scenario 3 simulates a winter condition, where the supply air temperature ranges from 24.1 to -6.87 °C and the radiant slabs run in cooling mode and heating mode, respectively. Due to the limited space in this paper, the comparison of vertical air temperature and velocity in these two scenarios will not be illustrated here. The effect of supply air temperature on the vertical temperature gradient of the conditioned space is not significant. The air temperature differences between head and ankle level are less than 0.4 °C in scenario 2 and less than 0.9 °C for scenario 3. However, the relative high velocity near the floor moves along the horizontal direction while the supply air temperature changes. In winter the cold downward flow generates a strong circulation close to the front wall. On the contrary, the warm supply air in summer allow a longer penetration length, thus, strong air circulation occurs at the end of the room. Generally, these two models give satisfactory prediction of the flow pattern in the conditioned space. Although the porous media model has smaller discrepancies to measured results, the difference between two models is quite limited.

Air distribution in the plenum and through diffuse ceiling

The thermal processes within the plenum have an important impact on the effectiveness of diffuse ceiling ventilation. An appropriate numerical model should be able to correctly predict the air flow pattern and thermal processes in the plenum and through the diffuse ceiling.

Figure 11 shows the relationship between plenum air temperature and the distance to plenum inlet in the three scenarios. As the air travels through the plenum, it is gradually warmed up or cooled down by heat transfer from the diffuse ceiling panels and from the radiant slabs, named as thermal decay. Both CFD models give acceptable predications on the thermal decay of plenum air. The largest disagreement occurs

in scenario 3, where the peak air temperature at the center is not predicted by the CFD models. This may be caused by a reverse flow occurring in this region due to the thermal plume from the heat sources. On the other hand, although the supply air temperature changes from -6.87 °C to 24.10 °C, the air temperature in the plenum stays relatively stable (14 °C to 22 °C). This indicates a significant pre-heating or pre-cooling effect of the plenum.

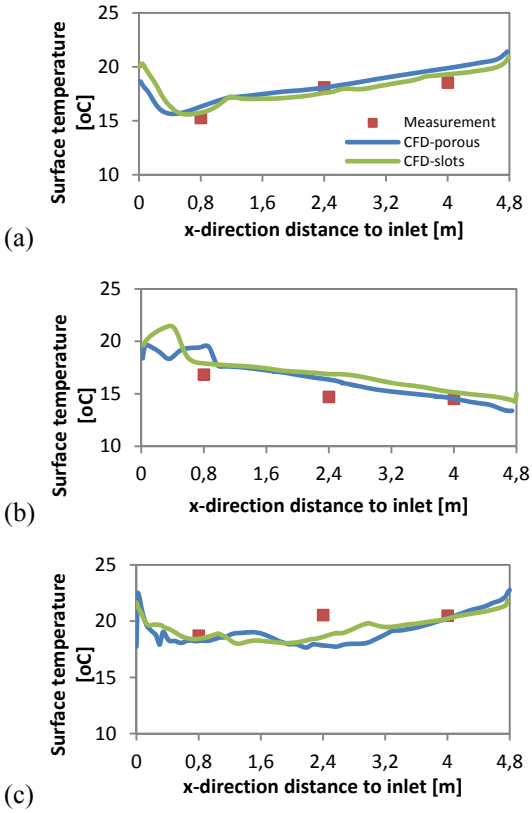

Figure 11 Plenum air temperature distribution (a) Scenario 1 (b) Scenario 2 (c) Scenario 3

As a medium between the plenum and the room, the diffuse ceiling panel has a complex heat exchange with these two zones. The diffuse ceiling surface temperatures are measured and simulated in the three scenarios, as presented by Figure 12. The measured data indicate that the surface temperatures are not uniformly distributed, but changes as a function of the distance to plenum inlet. In addition, a noticeable temperature difference between the diffuse ceiling lower and upper surface is observed, which reaches to 10 °C. The simplified geometrical model obtains a better agreement with the measured data, although the surface temperature drops in the positions, where the slot openings are built. The porous media model fails to predict the surface temperature of the diffuse ceiling panels, especially when the radiant slabs are activated (Scenario 2 and 3). This is because the porous media is treated as a fluid zone in the CFD software and the diffuse ceiling surfaces are regarded as interiors between two fluid zones. Therefore, instead of predicting surface temperature, the porous media model calculates the air temperature through the diffuse ceiling panels. On the other hand, because the porous media model is incompatible with the radiation model, the impact of radiation heat transfer to/from the diffuse ceiling panel is calculated and treated as an energy source term in the energy equation. These assumptions cause the disagreement between the CFD simulations and the experiments.

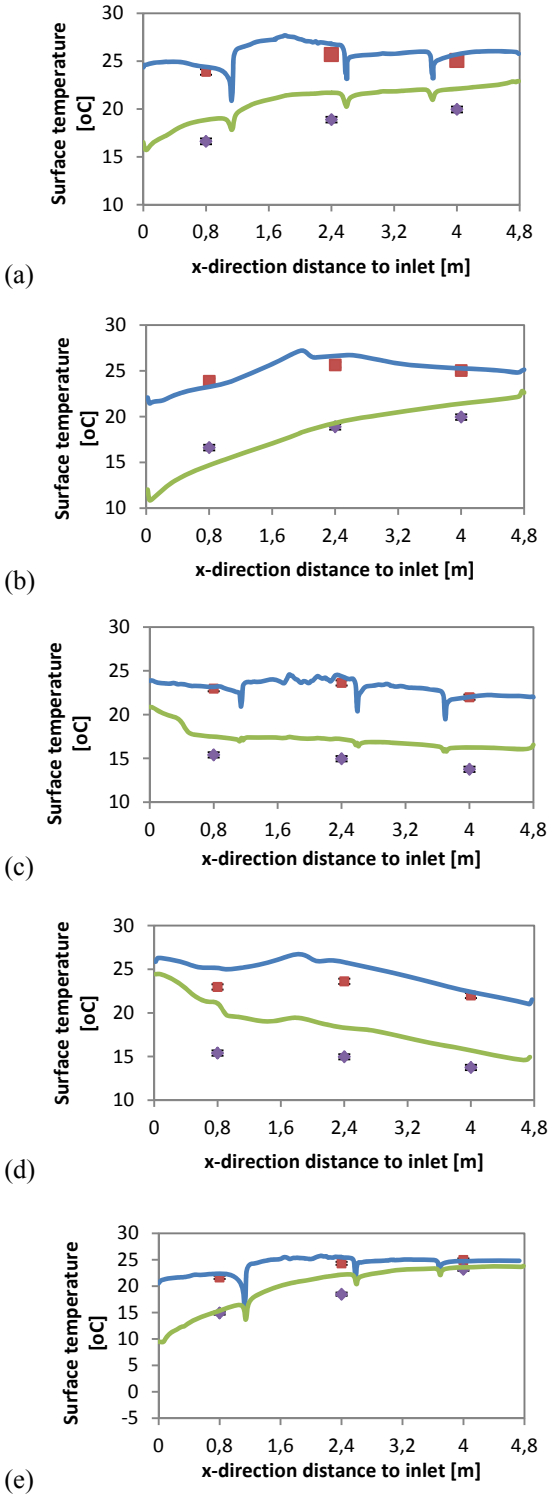

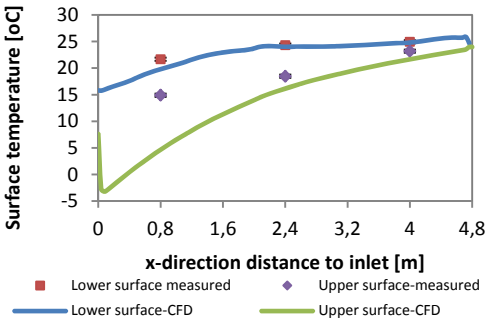

(f)

Figure 12 Diffuse ceiling surface temperature distribution. Scenario 1: (a) Simplified geometrical model (b) Porous media model; Scenario 2: (c) Simplified geometrical model (d) Porous media model; Scenario 3: (e) Simplified geometrical model (f) Porous media model

CONCLUSION

The objective of this research is to develop a simplified method on predicting the air flow pattern of diffuse ceiling ventilation in the CFD simulation. Two numerical models have been presented and compared, one is a simplified geometrical model and the other is a porous media model. The measured data obtained by the full-scale experiments are used to validate the numerical models.

Both the experimental results and the numerical results indicate that buoyancy flows generated by heat sources is the driving force for air distribution in a room with diffuse ceiling ventilation. The thermal plume increases the mixing level, creating a uniform temperature distribution in the occupied zone. A relative high velocity is observed at the ankle level near the front wall, however, no draught risk is predicted in any of the scenarios. A thermal decay of the supply air is observed in the plenum, due to the heat exchange between the air and the thermal mass (concrete slabs and diffuse ceiling panels). On the other hand, the plenum has a significant pre-heating or pre-cooling effect, enabling the air to be supplied into the room with an acceptable temperature.

Generally, the two numerical models reach good agreement with the measured data on the air temperature and velocity distribution in the occupied zone. The porous media model gives better predictions on the flow characteristic just through diffuse ceiling, and the air velocity near the floor. However, the simplified geometrical model shows superior performance on predicting the diffuse ceiling surface temperature. This is because of the limitations of the porous media model in the CFD software, where it is treated as a fluid zone and is incompatible with a radiation model.

REFERENCES

ANSYS, I. (2009). ANSYS FLUENT User's Guide.

Brohus, H., & Balling, K. D. (2004). Local Exhaust Efficiency in an Operating Room Ventilated by Horizontal Unidirectional Airflow. In Proceedings of Roomvent 2004. Coimbria Portugal.

Chen, Q. and A. Moser. (1991). Simulation of a Multiple-Nozzle Diffuser. Proceedings of 12th AIVC Con- ference 2:1-14.

Chodor, A. D., & Taradajko, P. P. (2013). Experimental and Numerical Analysis of Diffuse Ceiling Ventilation. Aalborg University.

Fan, J., Hviid, C. A., & Yang, H. (2013). Performance analysis of a new design of office diffuse ceiling ventilation system. Energy and Buildings, 59, 73–81.

Hviid, C. A. (2013). Numerical investigation of diffuse ceiling ventilation in an office under different operating conditions.

Hviid, C. A., & Svendsen, S. (2013). Experimental study of perforated suspended ceilings as diffuse ventilation air inlets. Energy and Buildings, 56, 160–168.

ISO 7730. (2005). Ergonomics of the thermal environment -- Analytical determination and interpretation of thermal comfort using calculation of the PMV and PPD indices and local thermal comfort criteria.

Jacobs, P., & Knoll, B. (2009). Diffuse ceiling ventilation for fresh classrooms. Proceedings of 4 th Intern. Symposium on Building and Ductwork Air tightness. Berlin, Germany.

Jacobsen, L. (2008). Air Motion and Thermal Environment in Pig Housing Facilities with Diffuse Inlet. Department of Civil Engineering, Aalborg University.

Lemaire, a. D., Chen, Q., Ewert, M., Heikkinen, J., Inard, C., Moser, a., … Whittle, G. (1993). IEA Annex 20: Air flow patterns within buildings. Room air and contaminant flow, evaluation of computational methods. Buildings, 82.

Nielsen, P. V, & Jakubowska, E. (2007). The Performance of Diffuse Ceiling Inlet and other Room Air Distribution Systems. Proceedings of Cold Climate HVAC 2009.Greenland.

Rong, L., Elhadidi, B., Khalifa, H. E., & Nielsen, P. V. (n.d.). CFD Modeling of Airflow in a Livestock Building. In IAQVEC 2010: The 7th International Conference on Indoor Air Quality, Ventilation and Energy Conservation in Buildings.

Skovgaard, M., Nielsen, P. V. (1991). Modelling Complex Inlet Geometries in CFD.

Srebric, J., & Chen, Q. (2003). Simplified numerical models for complex air supply diffusers. ASHRAE Transactions, 109 PART .